Mn substitution-driven structural and magnetic phase evolution in Bi1−xSmxFeO3 multiferroics

ARTICLE *in* JOURNAL OF APPLIED PHYSICS · JANUARY 2012

Impact Factor: 2.18 · DOI: 10.1063/1.3676205

4 AUTHORS, INCLUDING:

Vladimir Khomchenko
University of Coimbra
78 PUBLICATIONS **1,180** CITATIONS
SEE PROFILE

I. O. Troyanchuk
Belarusian State University
237 PUBLICATIONS **1,911** CITATIONS
SEE PROFILE

José António Paixão
University of Coimbra
450 PUBLICATIONS **2,413** CITATIONS
SEE PROFILE

AIP | Journal of Applied Physics

Mn substitution-driven structural and magnetic phase evolution in Bi1xSmxFeO3 multiferroics

V. A. Khomchenko, I. O. Troyanchuk, M. I. Kovetskaya, and J. A. Paixão

Citation: J. Appl. Phys. **111**, 014110 (2012); doi: 10.1063/1.3676205
View online: http://dx.doi.org/10.1063/1.3676205
View Table of Contents: http://jap.aip.org/resource/1/JAPIAU/v111/i1
Published by the American Institute of Physics.

Mn substitution-driven structural and magnetic phase evolution in $Bi_{1-x}Sm_xFeO_3$ multiferroics

V. A. Khomchenko,[1,a)] I. O. Troyanchuk,[2] M. I. Kovetskaya,[2] and J. A. Paixão[1]
[1]*CEMDRX/Department of Physics, Faculty of Sciences and Technology, University of Coimbra, 3004-516 Coimbra, Portugal*
[2]*SSPA "Scientific-Practical Materials Research Centre of NAS of Belarus," P. Brovka str. 19, 220072 Minsk, Belarus*

(Received 21 October 2011; accepted 28 November 2011; published online 12 January 2012)

X-ray diffraction and magnetization measurements of the $Bi_{0.9}Sm_{0.1}Fe_{1-y}Mn_yO_3$ and $Bi_{0.86}Sm_{0.14}Fe_{1-z}Mn_zO_3$ ($y \leq 0.4$, $z \leq 0.3$) series were carried out in order to follow the effect of Mn doping on the room temperature crystal structure and magnetic properties of Sm-substituted $BiFeO_3$. Initially polar rhombohedral $Bi_{0.9}Sm_{0.1}FeO_3$ compound (space group $R3c$) was shown to undergo the Mn-substitution driven structural transformation into the orthorhombic $Pnam$ phase at $y \sim 0.2$. Further increasing of the Mn content stabilizes the modified structural phase demonstrating the features of incommensurability. In the $Bi_{0.86}Sm_{0.14}Fe_{1-z}Mn_zO_3$ series, the initially dominant antipolar orthorhombic $Pnam$ phase transforms toward the nonpolar $Pnma$ structure ($z \sim 0.3$). Changes of the main magnetic state (from mixed antiferromagnetic/weak ferromagnetic to weak ferromagnetic) were found to correlate with the rhombohedral-to-orthorhombic transition; however, within the compositional range of the orthorhombically distorted compounds, the room temperature spontaneous magnetization rapidly decreases with increasing Mn content. [doi:10.1063/1.3676205]

I. INTRODUCTION

Magnetic ferroelectrics with a perovskite (ABO_3) structure have become the subject of numerous investigations.[1,2] The increased interest is explained by both the possibilities of practical applications of the magnetoelectric effect (induction of magnetization by an electric field or of electric polarization by a magnetic field) characteristic of some representatives of this class of materials and rich fundamental physics. Among multiferroic perovskites, $BiFeO_3$ is distinguished by its exceptionally high magnetic and ferroelectric transition temperatures ($T_N \approx 640$ K, $T_C \approx 1100$ K). In the ferroelectric phase, the compound has a rhombohedrally distorted structure with the space group $R3c$ (Ref. 3) and possesses a large polarization $P_S \sim 100\ \mu C/cm^2$ (Ref. 4) directed along the $[111]_c$ axis of the parent perovskite pseudocubic cell (along the $[001]_h$ axis in the hexagonal setting). The existence of polar ionic displacements is due to the stereochemical activity of the $6s^2$ lone pairs of Bi^{3+} ions. Superexchange interactions between magnetically active Fe^{3+} ions give rise to G-type antiferromagnetic ordering (that is, the magnetic moment of each Fe cation is antiparallel to that of its nearest neighbors). Due to the inhomogeneous magnetoelectric interaction,[5] the antiferromagnetic structure is modulated with a long-range (~620 Å) cycloid propagating along the $[110]_c$ direction.[6]

Despite having been intensively studied for many years,[7] the effect of a lanthanide (Ln) A-site substitution on the crystal structure and physical properties of $BiFeO_3$ has not been fully elucidated. The variety of the models describing the structural phase evolution in the $Bi_{1-x}Ln_xFeO_3$ series upon doping, as well as the drastic difference in the ferroelectric/magnetic behavior reported for doped compounds having a close chemical composition, seems to reflect a tendency of the materials toward structural phase separation.[8] The newly developed paradigm joining results of extensive structural characterization of the $Bi_{1-x}Ln_xFeO_3$ compounds with their multiferroic properties[8–17] suggests that an increasing lanthanide concentration in these series induces a number of the structural/ferroelectric/magnetic phase transitions to form the following sequence: the initial polar rhombohedral ($R3c$) antiferromagnet phase transforms into the intermediate antipolar orthorhombic ($Pnam$ for Ln = Pr, Nd, Sm, Eu, Gd,[10–14] or $Pnam$ and $Imma(00\gamma)s00$ for Ln = La (Refs. 8 and 9)) weak ferromagnetic phase which, in turn, transforms into the nonpolar orthorhombic weak ferromagnetic phase ($Pnma$) characteristic of $LnFeO_3$ orthoferrites. The decreasing ionic radius of substituting lanthanide shifts the concentration boundaries of the transitions toward smaller x to narrow stability ranges of the parent rhombohedral and intermediate orthorhombic phases.[8–14] The structural transformations occur as a first-order transition via the realization of a two-phase structural state.[8–14]

The crystal structure of $BiFeO_3$ is known to hardly accommodate any other magnetically active transition metal (M) ions in the B site of the ABO_3 perovskite, so conventional ceramic technology allows the $BiFe_{1-x}M_xO_3$ solid solutions to be obtained only in a rather limited compositional range. In particular, single-phase $BiFe_{1-x}Mn_xO_3$ perovskites can be realized for $x \leq 0.3$.[18] Mn substitution does not alter the space group of $BiFeO_3$ for $x \leq 0.3$, but it strongly decreases the temperatures of the ferroelectric and magnetic phase transitions.[18] The influence of simultaneous Ln and Mn substitution on the crystal structure and multiferroic

a)Author to whom correspondence should be addressed. Electronic mail: uladzimir@fis.uc.pt. Fax: +351 239 829 158.

behavior of $BiFeO_3$ perovskite is much less well studied, with the published data being rather contradictory. The results of the structural investigations undertaken for the $Bi_{0.9}La_{0.1}Fe_{1-x}Mn_xO_3$ ($x \leq 0.5$) series were interpreted in the model implying that all the compounds possessed the rhombohedral lattice with the space group $R3c$ (heavily doped samples contained impurity phases).[19] Structural characterization of $Bi_{0.9}Sm_{0.1}Fe_{1-x}Mn_xO_3$ ($x = 0.15,\ 0.3$) compounds showed that Mn substitution gave rise to the rhombohedral to orthorhombic $R3c \rightarrow Imma$ phase transition.[20] In order to contribute to a better understanding of the effect of the combined substitution on the structural and magnetic behavior of $BiFeO_3$, we performed solid state synthesis, x-ray diffraction, and magnetization measurements of a number of (Bi, Ln)$Fe_{1-x}Mn_xO_3$ series. In this paper, we report the results of the investigation carried out for samarium doped bismuth ferromanganites. In accordance with the structural phase diagram of the $Bi_{1-x}Sm_xFeO_3$ system,[10] 10% and 14% Sm-substituted series were chosen to follow the Mn-driven structural/magnetic phase evolution both for the initial $R3c$ and $Pnam$ phases.

II. EXPERIMENTAL

Polycrystalline samples of $Bi_{0.9}Sm_{0.1}Fe_{1-y}Mn_yO_3$ and $Bi_{0.86}Sm_{0.14}Fe_{1-z}Mn_zO_3$ ($y \leq 0.4$, $z \leq 0.3$) were prepared via a conventional solid-state reaction method using the high-purity oxides Bi_2O_3, Sm_2O_3 (annealed at 1000 °C), Fe_2O_3, and Mn_2O_3 taken in stoichiometric cation ratio and thoroughly mixed using a planetary mill (Retsch). The synthesis was carried out in air in a temperature range of 870−890 °C for 15 h (the annealing temperature was decreased with increasing Mn content). X-ray diffraction (XRD) patterns were collected at room temperature using a DRON-3 M diffractometer with CuKα radiation to be analyzed with the FULLPROF software package. Magnetic measurements were performed with a cryogen-free physical properties measurement system (Cryogenic Ltd.).

III. RESULTS AND DISCUSSION

The ideal perovskite (ABO_3) structure is composed of a three dimensional network of regular corner-linked octahedra BO_6. The B-site cations are at the center of the octahedra, with the A cations located in the body center of the cube formed by eight corner-linked octahedra. The symmetry of the ideal perovskite structure is cubic with the space group $Pm\bar{3}m$. Due to several types of distortions (octahedral tilting, polar or antipolar shifts of A- and/or B-ions from their exact position in the center of the octahedra or cuboctahedra, Jahn-Teller distortions) driven by the lattice and/or electronic instability, most perovskite-type compounds belong to lower symmetry groups. In $BiFeO_3$, the antiphase tilt of the adjacent FeO_6 octahedra ($a^-a^-a^-$ tilt system in Glazer's notation[21]) reduces the symmetry to the rhombohedral $R\bar{3}c$. The superimposed polar ionic displacements along the $[111]_c$ pseudocubic direction give the actual space group of $BiFeO_3$, $R3c$. For the $Bi_{0.9}Sm_{0.1}FeO_3$ compound, the polar rhombohedral structure is known to be retained.[10,22]

XRD study undertaken for samples of the $Bi_{0.9}Sm_{0.1}Fe_{1-y}Mn_yO_3$ series shows that 10% Mn substitution leaves the initial symmetry unaltered. Indeed, the corresponding diffraction pattern can be well fitted using the rhombohedral $R3c$ model with the unit cell parameters $a = b = \sqrt{2}a_c$ and $c = 2\sqrt{3}a_c$, where $a_c \approx 4$ Å is the parameter of the cubic perovskite subcell (Fig. 1(a)). Fitting of the spectrum obtained for the $Bi_{0.9}Sm_{0.1}Fe_{0.8}Mn_{0.2}O_3$ sample (Fig. 1(b)) indicates that the compound possesses the structure characteristic of the intermediate phase typically separating the polar $R3c$ and nonpolar $Pnma$ phases in the $Bi_{1-x}Ln_xFeO_3$ systems.[8–14] This structure is characterized by a $\sqrt{2}a_c \times 2\sqrt{2}a_c \times 4a_c$ supercell and combines $(a^-a^-c^+)/(a^-a^-c^-)$ octahedral tilting with $PbZrO_3$-like antipolar displacements of A-site cations along the $[110/\bar{1}\bar{1}0]_c$ directions of the parent cubic cell (space group $Pnam$; the nonstandard setting is used to distinguish this phase from that isostructural with $LnFeO_3$ perovskites (S.G. $Pnma$)). A very similar diffraction pattern was obtained for $y = 0.3$ samples (Fig. 1(c)). However, thorough analysis of the fitting did not confirm that all the observed diffraction peaks can be adequately described using the $Pnam$ model

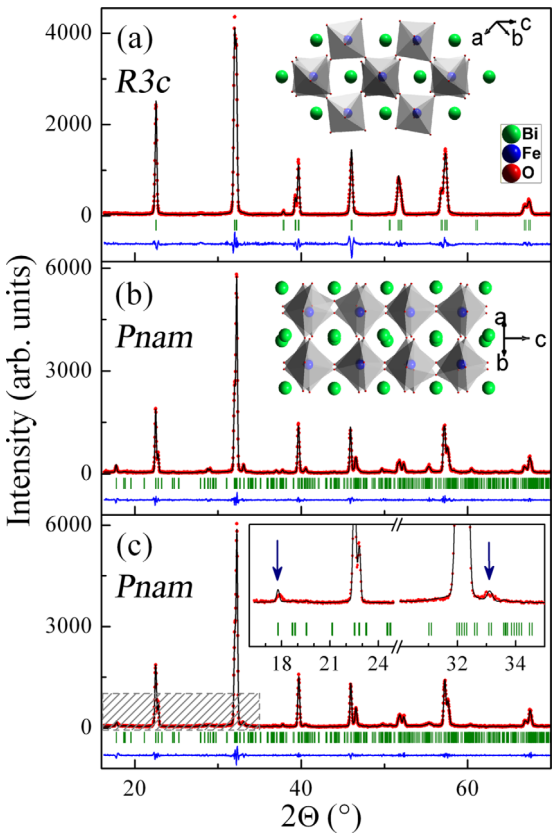

FIG. 1. (Color online) Observed, calculated, and difference XRD patterns for $Bi_{0.9}Sm_{0.1}Fe_{1-y}Mn_yO_3$ compounds: (a) $y = 0.1$ [S.G. $R3c$; $a = b = 5.5579(1)$ Å, $c = 13.7576(1)$ Å], (b) $y = 0.2$ [S.G. $Pnam$; $a = 5.5767(3)$ Å, $b = 11.1952(4)$ Å, $c = 15.5993(7)$ Å], and (c) $y = 0.3$ [the fitting taken in approximation of the $Pnam$ model with the cell parameters $a = 5.5768(3)$ Å, $b = 11.1841(5)$ Å, and $c = 15.5948(8)$ Å]. Bragg reflections are indicated by ticks. Insets of (a) and (b) show schematic views of the corresponding unit cells along the directions coincident with one of the main axes of the parent cubic perovskite cell. Inset of (c) shows enlarged parts of the diffraction spectra for the $y = 0.3$ sample to demonstrate insufficient agreement of the theoretical pattern given by the commensurate $Pnam$ model with the experimental peaks (marked with arrows).

(see inset in Fig. 1(c)). The same picture—when basic perovskite reflections are consistent with the $\sqrt{2}a_c \times 2a_c \times \sqrt{2}a_c$ orthorhombic unit cell, whereas small superlattice reflections are not compatible with any multiple supercell—has been detected in the XRD study of $Bi_{1-x}La_xFeO_3$ $(0.2 < x < 0.5)$ perovskites.[9] It was suggested that the observed features could be associated with the modulation of antipolar ordering.[9] Parallel electron microscopy and synchrotron x-ray diffraction investigations confirmed the formation of an incommensurately modulated structure with the superspace group $Imma(00\gamma)s00$.[8] It was shown that the primary modulation is caused by a displacement of the Bi and O atoms along the $[110]_c$ direction. The displacements have a polar character (i.e., create a local electric dipole, associated with the chain of the Bi and O atoms running along the $[110]_c$ direction). Intra-layer ordering of the dipole chains is mutually compensative and results in an antipolar structure. Local fluctuations of the intra-layer ordering are compensated for by interaction with the neighboring layers to yield incommensurability. The secondary modulation occurs because of displacement of the oxygen atoms that locally gives the in-phase octahedral tilt component added to the $a^-b^0a^-$ tilt system of the average *Imma* structure. It was concluded that the coupling of the polar displacements and the b^+ octahedral tilt through the lattice strain could be the driving force for the incommensurability in $Bi_{1-x}La_xFeO_3$.[8] The same main structural motif is retained for the $Bi_{0.9}Sm_{0.1}Fe_{0.6}Mn_{0.4}O_3$ compound: even though the intensity of the superlattice reflections incompatible with the commensurate *Imma* structure decreases, the diffraction experiment still easily detects them. Traces of the impurity phases $Bi_{25}(Fe,Mn)O_{39}$ and $Bi_2(Fe,Mn)_4O_9$ found in the diffraction spectrum of $y = 0.4$ samples imply that the chosen concentration of manganese slightly exceeds its solid solubility limit in the $Bi_{0.9}Sm_{0.1}Fe_{1-x}Mn_xO_3$ series.

Recent investigation of the $Bi_{0.86}La_{0.14-x}Sm_xFeO_3$ system revealed the coexistence of the orthorhombic *Pnam* (~63%) and rhombohedral *R*3*c* (~37%) phases in the $Bi_{0.86}Sm_{0.14}FeO_3$ compound.[17] Mn substitution in the $Bi_{0.86}Sm_{0.14}Fe_{1-z}Mn_zO_3$ series is found to stabilize the *Pnam* structure: the x-ray diffraction pattern obtained for the $Bi_{0.86}Sm_{0.14}Fe_{0.9}Mn_{0.1}O_3$ solid solution can be successfully fitted using a single-phase *Pnam* model (Fig. 2(a)). A further increase in the Mn content results in a gradual suppression of the diffraction peaks originating from the antipolar ionic displacements and the modulated in-phase/antiphase octahedral tilting, thus reflecting a tendency toward transformation of the *Pnam* symmetry to the orthorhombic *Imma* structure with the $\sqrt{2}a_c \times 2a_c \times \sqrt{2}a_c$ supercell and $a^-b^0a^-$ tilting scheme. However, in contrast to the results of Saxin and Knee,[20] the commensurate *Imma* structure was not reliably confirmed to exist in this series: even at $z = 0.2$, where the main perovskite phase starts to compete with the *Pnma* phase (the latter structure was found to be typical of compounds with a higher Mn concentration; in the $z = 0.2$ compound, its reflections can be traced on the background level), the peaks characteristic of *Pnam* structure do not disappear (Fig. 2(b)). At $z = 0.3$, the nonpolar orthorhombic *Pnma* structure that possesses the $\sqrt{2}a_c \times 2a_c \times \sqrt{2}a_c$ supercell and demonstrates a tilting distortion corresponding to Glazer's tilt system

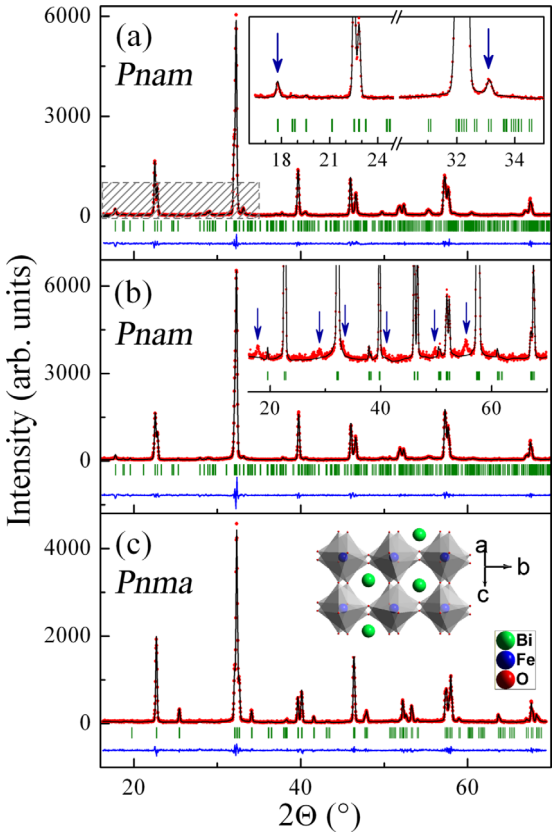

FIG. 2. (Color online) Observed, calculated, and difference XRD patterns for $Bi_{0.86}Sm_{0.14}Fe_{1-z}Mn_zO_3$ compounds: (a) $z = 0.1$ [S.G. *Pnam*; $a = 5.5742(3)$ Å, $b = 11.1862(5)$ Å, $c = 15.5865(8)$ Å; inset shows enlarged parts of the same spectra demonstrating good agreement between the experimental and theoretical patterns], (b) $z = 0.2$ [S.G. *Pnam*; $a = 5.5698(3)$ Å, $b = 11.1660(5)$ Å, $c = 15.5877(8)$ Å; inset shows the alternative fitting taken with the space group *Imma*; the peaks indescribable within the *Imma* model are marked with arrows], and (c) $z = 0.3$ [S.G. *Pnma*; $a = 5.5775(2)$ Å, $b = 7.8324(3)$ Å, $c = 5.4894(2)$ Å; inset shows schematic view of the corresponding unit cell along the direction coincident with one of the main axes of the parent cubic perovskite cell].

$a^-b^+a^-$ was proven to be realized (Fig. 2(c)). The structural parameters of the compounds under study are summarized in Figs. 3 and 4. One can see that *R*3*c* → *Pnam* and *Pnam* → *Pnma* crossovers are accompanied by a step-like contraction of the primitive cell volume characteristic of first-order transitions (Fig. 4). Beyond the transitions, the primitive cell volume gradually decreases with increasing Mn concentration (Fig. 4). The decreasing is likely associated with the changing oxidation state of Mn ions. Indeed, when synthesized in an open environment, manganese containing perovskites $AMnO_3$ $(A = Ln^{3+}, Bi^{3+})$ easily accommodate superstoichiometric oxygen;[18,23] the oxygen nonstoichiometry is realized via the formation of cation vacancies at *A* and *B* sites.[24] Accordingly, the defect chemistry of the nonstoichiometric $AMnO_{3+\delta}$ is actually described as $A_{1-\varepsilon}Mn_{1-\varepsilon}O_3$, where $\varepsilon = \delta/(3+\delta)$. Charge balance in $AMnO_{3+\delta}$ is achieved via oxidation of Mn^{3+} to Mn^{4+} in accordance with the expression $AMn^{3+}_{1-2\delta}Mn^{4+}_{2\delta}O_{3+\delta}$. Being a smaller ion,[25] Mn^{4+} provokes contraction of the cell parameters.

Cation vacancies and the changing oxidation state of manganese can effectively influence the crystal structure of the perovskite compounds. For instance, in the $BiMnO_{3+\delta}$

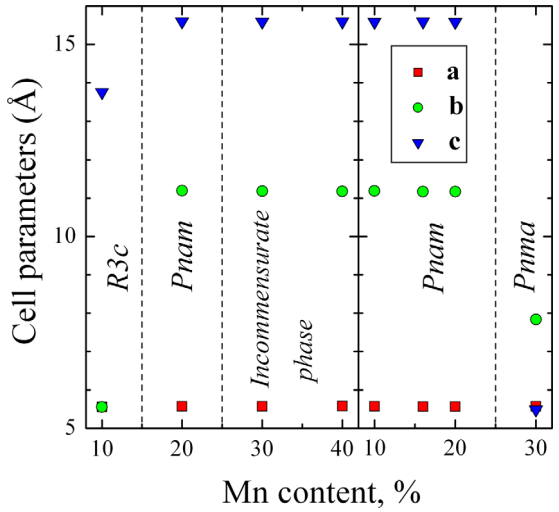

FIG. 3. (Color online) Compositional dependences of the unit cell parameters for $Bi_{0.9}Sm_{0.1}Fe_{1-y}Mn_yO_3$ (left panel) and $Bi_{0.86}Sm_{0.14}Fe_{1-z}Mn_zO_3$ (right panel) series. Dashed lines separate concentration ranges of the distinct structural phases. For the incommensurate phase, the parameters were taken in approximation of the *Pnam* model.

series, an increasing oxygen concentration (in other words, increasing cation vacancy concentration/increasing Mn^{4+} ion content) gives rise to the transition sequence $C2/c \rightarrow P2_1/c \rightarrow Pnma$; charge-ordering and vacancy-ordering scenarios are suggested as possible reasons for the $C2/c \rightarrow P2_1/c$ crystal symmetry change.[26] However, oxygen nonstoichiometry is probably not the only factor that might affect the stability of the initial phase of the (Bi, Sm)(Fe, Mn)$O_{3+\delta}$ compounds upon Mn doping. Indeed, though investigation of the $BiFe_{1-x}Mn_xO_{3+\delta}$ ($x = 0.1$, 0.2) solid solutions revealed an evident tendency toward decreasing ferroelectric Curie temperature with increasing Mn concentration (6 to 7 °C per 1% Mn), they showed a rather weak dispersion of the T_C

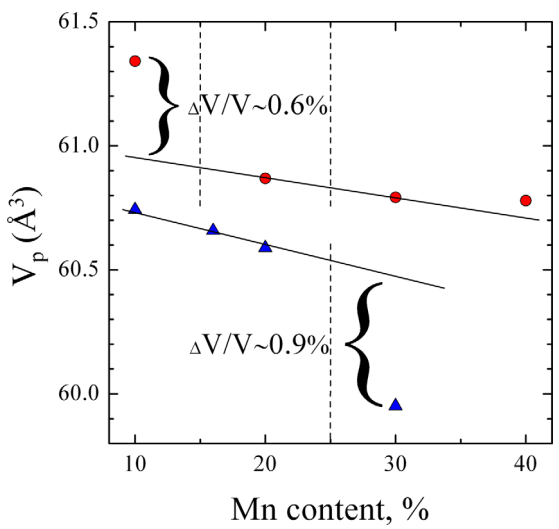

FIG. 4. (Color online) Compositional dependences of the primitive cell volume for $Bi_{0.9}Sm_{0.1}Fe_{1-y}Mn_yO_3$ (red circles) and $Bi_{0.86}Sm_{0.14}Fe_{1-z}Mn_zO_3$ (blue triangles) series. Straight lines reflecting a Vegard's law behavior are drawn as guides for the eye. The point corresponding to the nominal composition $y = 0.4$ was not included in the linear fit because the sample contains impurity phases. Dashed lines separate concentration ranges of the distinct structural phases.

with changing oxygen content (varying in the range $0.015 \leq \delta \leq 0.028$ for $x = 0.1$ and $0.016 \leq \delta \leq 0.037$ for $x = 0.2$).[18] This fact could be explained by the small Mn content and, correspondingly, by a low concentration of related defects (cation vacancies, Mn^{4+} ions) that is insufficient to compete with some other factor determining decreasing T_C upon Mn doping. Indeed, the oxygen nonstoichiometry-related variation of the Curie point becomes more pronounced for $x = 0.3$ samples.[18] Surprisingly, the lowest transition temperatures were obtained for the most oxidized ($\delta = 0.059$) and *stoichiometric* ($\delta = 0$) compounds. The latter result is puzzling because Fe^{3+} and Mn^{3+} ions have equal ionic radii in octahedral coordination[25] (this fact is consistent with the direct estimation of the structural parameters of the $BiFeO_3$ and $BiFe_{0.7}Mn_{0.3}O_3$ compounds that were found to be expectedly close[18]). Accordingly, there is no evident lattice-related driving force that might be responsible for destabilizing the polar structure of $BiFeO_3$. On the other hand, Mn^{3+} ($t_{2g}^3 e_g^1$) are known to be Jahn-Teller ions, so the dynamic local distortions of the oxygen octahedra required in order to remove the electronic degeneracy[27] might be considered as a possible factor determining the structural instability (i.e., substantially lowering the Curie point) in the near-stoichiometric $BiFe_{1-x}Mn_xO_3$ compounds. In (Bi, Sm)(Fe, Mn)$O_{3+\delta}$ systems, local disorder in the arrangement of the lone pairs $6s^2(Bi^{3+})$ introduced by the lanthanide substitution must destabilize the cooperative dipole ordering characteristic of $BiFeO_3$, so the simultaneous introduction of Mn ions into Fe sites leads to the much more pronounced response from the side of a crystal lattice. Our investigations of Mn-substituted $Bi_{1-x}La_xFeO_3$ and $Bi_{1-x}Pr_xFeO_3$ series (which will be reported elsewhere) are consistent with the results of the present work and show that both initial polar rhombohedral and intermediate antipolar orthorhombic structures characteristic of the low-doped $Bi_{1-x}Ln_xFeO_3$ (Refs. 8, 9, and 11) can be effectively modified by Mn substitution to stabilize new phases either demonstrating the traits of incommensurability or possessing a nonpolar structure. The results indicate the important role of the B-sublattice order in the stabilization of an electric dipole ordering (driven by stereochemical activity of Bi^{3+} lone pair electrons) in lanthanide-substituted $BiFeO_3$. It is interesting to note that the oxygen-stoichiometric $BiFe_{1-x}Mn_xO_3$ system synthesized under high pressure and, thus, demonstrating a common trend of the structural changes at nonequilibrium conditions undergoes the structural phase transformation at $x \sim 0.2$.[28] The substitution-induced phase stable at $0.2 \leq x \leq 0.6$ has an orthorhombic $\sqrt{2}a_c \times 2\sqrt{2}a_c \times 4a_c$ unit cell.[28] The most recent investigations of the $BiFe_{1-x}Mn_xO_3$ series confirm that the high-pressure phase possesses the $PrZrO_3$-like *Pnam* structure.[29]

$BiFeO_3$ is known to have a cycloid-modulated antiferromagnetic structure in which the magnetic moments of Fe^{3+} ions locally retain their antiferromagnetic *G*-type orientation and rotate along the propagation direction of the modulated wave in the plane perpendicular to the hexagonal basal plane.[6] Such a modulation prevents the observation of weak ferromagnetism allowed by symmetry of the space group *R*3*c*,[30] so the field dependence of the magnetization characteristic of the stoichiometric compound demonstrates a linear character for

fields H of up to 60 to 70 kOe (at room temperature), at which point progressive deviation from the linearity starts to develop.[11,15,31] The behavior is associated with the field-induced transition from the spatially modulated antiferromagnetic structure to a homogeneous weak ferromagnetic state, which completely stabilizes above $H \sim 200$ kOe.[32] Within the concentration range of the rhombohedral $Bi_{1-x}Ln_xFeO_3$ compounds, an increasing lanthanide content results in a magnetic anisotropy change-driven decrease of the threshold field of the induced phase transition[11,15,31,32] and the appearance of a very small remanent magnetization (the latter was explained by *local* suppression of the initial spatial spin modulation induced by local deviation from a homogeneous distribution of the substituting elements or/and lattice defects[9,17]). In the rhombohedral phase, manganese substitution does not alter the dominant room-temperature magnetic behavior, so $y = 0.1$ samples demonstrate magnetization versus magnetic field dependency very typical of low-doped $Bi_{1-x}Ln_xFeO_3$ (Fig. 5(a)).[9,11,17,22] The magnetic state of the $Bi_{0.9}Sm_{0.1}Fe_{1-y}Mn_yO_3$ series changes upon the concentration transition into the orthorhombic phase (Fig. 5(b)). The field dependence of the magnetization obtained for the $y = 0.2$ compound demonstrates behavior characteristic of weak ferromagnets. A significant increase of the remanent magnetization and the coercive field is observed. However, the spontaneous magnetic moment is approximately two times smaller than that typical of manganese-free orthorhombic $Bi_{1-x}Ln_xFeO_3$ ($M_s \sim 0.25$ to 0.3 emu/g).[9,11,12,22] The appearance/enhancement of the spontaneous magnetization taking place in the $Bi_{0.9}Sm_{0.1}Fe_{1-y}Mn_yO_3$ system upon the $R3c \rightarrow Pnam$ transition is associated with the concomitant suppression of the incommensurate G-type antiferromagnetic order.[33] It is widely accepted that the net magnetization in orthorhombic phases of $Bi_{1-x}Ln_xFeO_3$ compounds is due to the antisymmetric spin-spin interaction of the form $\mathbf{D}\cdot(\mathbf{S}_1 \times \mathbf{S}_2)$, where $\mathbf{D}$ is the so-called Dzyaloshinsky vector (the microscopic origin of this term is attributed to the anisotropic superexchange interaction including spin-orbital coupling).[34,35] Weak ferromagnetic dependences are also observed for $y = 0.3$ and $y = 0.4$ samples (Fig. 5(b)). However, within the compositional range of the orthorhombically distorted compounds, the remanent magnetization and coercive field steadily decrease with increasing Mn concentration. The behavior is consistent with the Neel point decrease observed in the $BiFe_{1-x}Mn_xO_3$ (Ref. 18) and $Bi_{0.9}Sm_{0.1}Fe_{1-x}Mn_xO_3$ (Ref. 20) systems (~4 to 7 °C per 1% Mn, depending on the oxygen stoichiometry) with increasing manganese concentration (the Dzyaloshinsky-Moriya interaction is proportional to the exchange interaction). Very similar results were obtained with the room temperature magnetic characterization of the (Bi, Pr)(Fe, Mn)O_3 series (the results will be reported elsewhere), implying the realization of a common trend characteristic of lanthanide substituted $BiFeO_3$ upon Mn doping.

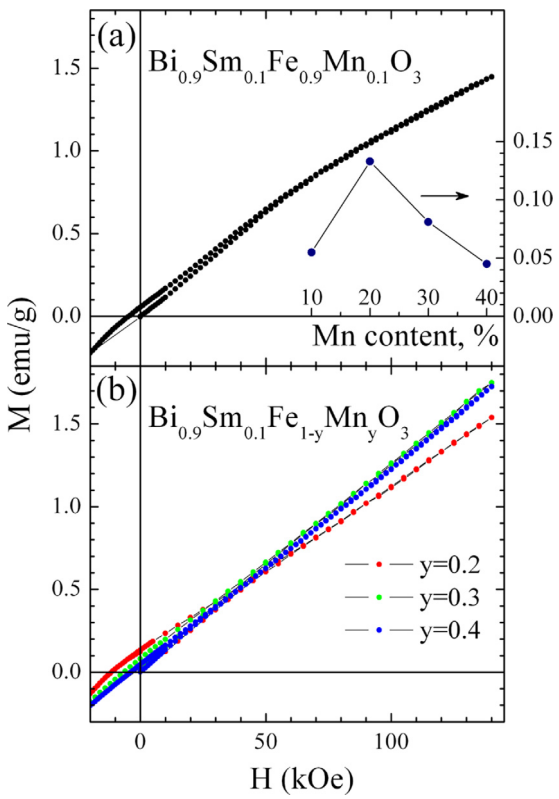

FIG. 5. (Color online) Field dependences of the magnetization obtained for $Bi_{0.9}Sm_{0.1}Fe_{1-y}Mn_yO_3$ compounds at room temperature: (a) $y = 0.1$, (b) $0.2 \leq y \leq 0.4$. Inset shows the compositional dependence of the remanent magnetization.

IV. CONCLUSIONS

Solid state synthesis and investigation of the crystal structure and magnetic properties of $Bi_{0.9}Sm_{0.1}Fe_{1-y}Mn_yO_3$ and $Bi_{0.86}Sm_{0.14}Fe_{1-z}Mn_zO_3$ ($y \leq 0.4$, $z \leq 0.3$) perovskites were performed. Mn substitution was found to effectively modify both the initial polar rhombohedral and intermediate antipolar orthorhombic structures characteristic of low-doped $Bi_{1-x}Sm_xFeO_3$ (Refs. 10, 16, and 22) to stabilize the new phases either demonstrating the traits of incommensurability or possessing a nonpolar structure. In the rhombohedral phase, manganese substitution does not alter the dominant room-temperature magnetic interactions characteristic of the isostructural $Bi_{1-x}Ln_xFeO_3$ perovskites,[9,11,17,22] and the corresponding samples demonstrate the behavior expected for a mixed antiferromagnetic/weak ferromagnetic state. The magnetic state in the Mn-containing series changes upon the concentration transition into the orthorhombic phase. The orthorhombic compounds possess magnetic properties compatible with weak ferromagnetism. Their room temperature spontaneous magnetization steadily decreases with increasing Mn content.

ACKNOWLEDGMENTS

This work is supported by funds from FEDER (Programa Operacional Factores de Competitividade COMPETE) and from FCT-Fundação para a Ciência e a Tecnologia under project PEst-C/FIS/UI0036/2011 and the "Ciência 2008" program. The authors would also like to acknowledge the financial support of the BRFFI (Grant No. T10R-119).

[1]M. Fiebig, J. Phys. D: Appl. Phys. **38**, R123 (2005).
[2]S. Picozzi and C. Ederer, J. Phys.: Condens. Matter **21**, 303201 (2009).

[3]F. Kubel and H. Schmid, Acta Crystallogr., Sect. B: Struct. Sci. **46**, 698 (1990).
[4]D. Lebeugle, D. Colson, A. Forget, and M. Viret, Appl. Phys. Lett. **91**, 022907 (2007).
[5]A. K. Zvezdin and A. P. Pyatakov, Phys. Usp. **52**, 845 (2009).
[6]I. Sosnowska, T. Peterlin-Neumaier, and E. Steichele, J. Phys. C **15**, 4835 (1982).
[7]Z. V. Gabbasova, M. D. Kuz'min, A. K. Zvezdin, I. S. Dubenko, V. A. Murashov, D. N. Rakov, and I. B. Krynetsky, Phys. Lett. A **158**, 491 (1991).
[8]D. A. Rusakov, A. M. Abakumov, K. Yamaura, A. A. Belik, G. Van Tendeloo, and E. Takayama-Muromachi, Chem. Mater. **23**, 285 (2011).
[9]I. O. Troyanchuk, D. V. Karpinsky, M. V. Bushinsky, V. A. Khomchenko, G. N. Kakazei, J. P. Araujo, M. Tovar, V. Sikolenko, V. Efimov, and A. L. Kholkin, Phys. Rev. B **83**, 054109 (2011).
[10]S. Karimi, I. M. Reaney, Y. Han, J. Pokorny, and I. Sterianou, J. Mater. Sci. **44**, 5102 (2009).
[11]V. A. Khomchenko, I. O. Troyanchuk, D. V. Karpinsky, and J. A. Paixão, J. Mater. Sci. **47**, 1578 (2012).
[12]I. Levin, M. G. Tucker, H. Wu, V. Provenzano, C. L. Dennis, S. Karimi, T. Comyn, T. Stevenson, R. I. Smith, and I. M. Reaney, Chem. Mater. **23**, 2166 (2011).
[13]S. B. Emery, C.-J. Cheng, D. Kan, F. J. Rueckert, S. P. Alpay, V. Nagarajan, I. Takeuchi, and B. O. Wells, Appl. Phys. Lett. **97**, 152902 (2010).
[14]V. A. Khomchenko, I. O. Troyanchuk, M. V. Bushinsky, O. S. Mantytskaya, V. Sikolenko, and J. A. Paixão, Mater. Lett. **65**, 1970 (2011).
[15]G. Le Bras, P. Bonville, D. Colson, A. Forget, N. Genand-Riondet, and R. Tourbot, Physica B **406**, 1492 (2011).
[16]V. A. Khomchenko, J. A. Paixão, B. F. O. Costa, D. V. Karpinsky, A. L. Kholkin, I. O. Troyanchuk, V. V. Shvartsman, P. Borisov, and W. Kleemann, Cryst. Res. Technol. **46**, 238 (2011).
[17]V. A. Khomchenko, L. C. J. Pereira, and J. A. Paixão, J. Phys. D: Appl. Phys. **44**, 185406 (2011).
[18]S. M. Selbach, T. Tybell, M.-A. Einarsrud, and T. Grande, Chem. Mater. **21**, 5176 (2009).
[19]A. Ianculescu, F. Prihor, P. Postolache, L. Mitoseriu, N. Dragan, and D. Crisan, Ferroelectrics **391**, 67 (2009).
[20]S. Saxin and C. S. Knee, Dalton Trans. **40**, 3462 (2011).
[21]A. M. Glazer, Acta Crystallogr., Sect. A: Cryst Phys., Diffr., Theor. Gen. Crystallogr. **31**, 756 (1975).
[22]V. A. Khomchenko, J. A. Paixão, V. V. Shvartsman, P. Borisov, W. Kleemann, D. V. Karpinsky, and A. L. Kholkin, Scr. Mater. **62**, 238 (2010).
[23]V. A. Khomchenko, I. O. Troyanchuk, O. S. Mantytskaya, M. Tovar, and H. Szymczak, J. Exp. Theor. Phys. **103**, 54 (2006).
[24]J. A. M. Van Roosmalen, E. H. P. Cordfunke, R. B. Helmholdt, and H. W. Zandbergen, J. Solid State Chem. **110**, 100 (1994).
[25]R. D. Shannon, Acta Crystallogr., Sect. A: Cryst Phys., Diffr., Theor. Gen. Crystallogr. **32**, 751 (1976).
[26]A. A. Belik, K. Kodama, N. Igawa, S.-I. Shamoto, K. Kosuda, and E. Takayama-Muromachi, J. Am. Chem. Soc. **132**, 8137 (2010).
[27]J. Kanamori, J. Appl. Phys. **31**, 14S (1960).
[28]M. Azuma, H. Kanda, A. A. Belik, Y. Shimakawa, and M. Takano, J. Magn. Magn. Mater. **310**, 1177 (2007).
[29]A. A. Belik, A. M. Abakumov, A. A. Tsirlin, J. Hadermann, J. Kim, G. Van Tendeloo, and E. Takayama-Muromachi, Chem. Mater. **23**, 4505 (2011).
[30]C. Ederer and N. A. Spaldin, Phys. Rev. B **71**, 060401 (2005).
[31]G. Le Bras, D. Colson, A. Forget, N. Genand-Riondet, R. Tourbot, and P. Bonville, Phys. Rev. B **80**, 134417 (2009).
[32]A. M. Kadomtseva, Yu. F. Popov, A. P. Pyatakov, G. P. Vorob'ev, A. K. Zvezdin, and D. Viehland, Phase Transitions **79**, 1019 (2006).
[33]D. P. Kozlenko, A. A. Belik, A. V. Belushkin, E. V. Lukin, W. G. Marshall, B. N. Savenko, and E. Takayama-Muromachi, Phys. Rev. B **84**, 094108 (2011).
[34]I. Dzyaloshinsky, J. Phys. Chem. Solids **4**, 241 (1958).
[35]T. Moriya, Phys. Rev. **120**, 91 (1960).